Crystal Structure of Melaminium Orthophosphate from High-Resolution Synchrotron Powder-Diffraction Data

by **Dirk J. A. De Ridder***, **Kees Goubitz**, **Vladimir Brodski**, **René Peschar**, and **Henk Schenk**

Laboratory for Crystallography, van 't Hoff Institute for Molecular Sciences, Faculty of Science, University of Amsterdam, Nieuwe Achtergracht 166, NL-1018 WV Amsterdam (phone: +31-20-525-7039; fax: +31-20-525-6940; e-mail: dirkdr@science.uva.nl)

The crystal structure of melaminium orthophosphate (MP) has been determined from high-resolution synchrotron powder-diffraction data. The crystal packing consists of melaminium layers and pairs of orthophosphate chains connected by H-bonds almost perpendicular to the layers. The distance between melaminium layers is 3.62 Å. Neighboring melaminium molecules do not lie in the same plane, but in two parallel planes at close distance (0.79 Å), and are shifted with respect to each other. The orthophosphate chains are connected by both intra-chain and inter-chain H-bonds. The melamine is singly protonated at an endocyclic N-atom. The powder-diffraction data were corroborated by solid-state NMR experiments.

1. Introduction. – One of the performance characteristics of bulk polymers and engineering plastics is their flammability. Most of the widely applied polymers are not intrinsically fire-resistant and burn completely upon ignition. However, in many applications, for example, electric and electronic appliances and consumer products, the flammability of the polymers must be reduced for safety reasons. In general, this is accomplished by addition of so-called flame retardants (FRs). Nowadays, the market of FRs is for a large part dominated by health- and environmentally hazardous materials like halogenated compounds. Brominated FRs, for example, are a source of extremely toxic brominated dioxins and furans [1]. Also, from a technical viewpoint, halogenated FRs are highly disadvantageous: the formation of very corrosive gases like HBr, especially during the burning process, causes more damage than the actual fire, by affecting, *e.g.*, electronic equipment.

Several years ago, *DSM* (Geleen, The Netherlands) and *Ciba Specialty Chemicals* (Basel, Switzerland) started with the development of halogen-free FRs based on melamine (=1,3,5-triazine-2,4,6-triamine) [2]. Melamine cyanuric acid [3], for example, was developed for a specific polymer: *polyamide 6*. The use of melamine at large scale for fire-retarding applications is, however, quite limited. This can be attributed mainly to the lack of fundamental knowledge on the flame-retarding mechanism of nonhalogen FRs in general, and melamine-based systems in particular. Knowledge concerning the molecular and crystal structure is, thus, expected to improve the optimization of the thermal stability of the product.

Melamine readily forms insoluble adducts with many organic and inorganic acids [4]. Melamine is also used as an agent for producing linear and cyclic polyphosphate compounds [5]. In the framework of a project to establish the structural characteristics of environmentally friendly FRs based on melamine and its derivatives, we have now

determined the crystal structure of melaminium orthophosphate (MP). Since it has not been possible to grow suitable single crystals, the crystal structure had to be determined on the basis of powder-diffraction data.

2. Results and Discussion. – 2.1. *Protonation of Melamine.* It is well known that X-ray structure elucidations are limited with respect to the determination of H-atom positions. Therefore, before performing the *Rietveld* refinement, the question of the number and precise position of the H-atom(s) bonded to the melamine N-atom(s) had to be addressed. Melamine can be protonated either at the endocyclic N-atoms in the triazene ring or the exocyclic NH_2 groups. Based on UV-absorption experiments, *Hirt* and *Schmitt* [6] predicted that the endocyclic N-atoms are more basic than the NH_2 groups. Preferred ring protonation was also suggested by molecular-orbital (MO) calculations. Using *Hückel* theory, *Morimoto* showed the ring-protonated form of melamine to have a lower π-electron energy than the NH_2-protonated form [7]. Ring-protonated forms were considered in order to establish a correlation between the pK_a values and the electronic-energy levels and atomic charges as obtained from simple MO computations on various amino-oxo derivatives of 1,3,5-triazine [8]. Without argumentation, protonation of the triazine N-atoms was also assumed by *Albert* and co-workers [9], and by *Korolev* and *Mal'tseva* [10]. Energy calculations by the CNDO/2 method of two monocation and four dication models of melamine indicated that melamine, in acidic aqueous solution, is most likely a monocation with a proton attached to an endocyclic N-atom [11]. MO Calculations with MOSP, combining the *Hückel* with the *Del Re* method, indicated the triazine N-atoms of melamine to have a higher negative charge and to contribute more to the highest-occupied molecular orbital (HOMO) than the NH_2 N-atoms [12]. Finally, the IR spectra of different melamine/acid adducts (including those with H_3PO_4) showed the formation of salts with a high concentration of C=N bonds, indicating ring-N-atom protonation [13]. Only *Jahagirdar* and *Kharwadkar* appear to have taken for granted that protonation of melamine occurs at the NH_2 group(s) [14], although they only discussed in detail the degree of protonation, but not the position.

Protonation of a second triazine N-atom of melamine is less likely than protonation of the first one, and triple protonation is even more unlikely than double protonation. The number of protonated N-atoms is strongly dependent on the environment. Potentiometric and conductometric titrations in H_2O, DMSO and H_2O/DMSO mixtures have revealed that only one N-atom gets protonated in H_2O, all N-atoms get protonated simultaneously in DMSO (mol fraction close to unity), and two N-atoms get protonated in a stepwise process in DMSO/H_2O mixtures (for a DMSO mol-fraction-range of 0.38–0.78) [14].

The position(s) and degree of protonation of endo- and/or exocyclic melamine-N-atoms are suggested by the crystal structures retrieved from the *Cambridge Structural Database* [15]: next to melamine, only singly or doubly charged melaminium adducts are found. In the cation cases, melamine is exclusively protonated at one or two endocyclic N-atoms.

2.2. *Crystal-Structure-Determination*. The unit-cell parameters determined and refined (*Table 1*), initially using *Guinier* data and later on synchrotron data, are different from those reported by *Frazier et al.* [16]. The *d* values obtained in this latter

Table 1. *Experimental Details of the X-Ray Powder-Diffraction Structure of Melaminium Orthophosphate* (MP). Synchrotron radiation, $\lambda = 0.75003$ Å.

Molecular formula	$C_3H_7N_6^+ \cdot H_2PO_4^-$
M_r [g mol^{-1}]	224.12
Cell setting, space group	Triclinic, $P\bar{1}$ (No. 2)
Z	2
Lattice constants:	
a [Å]	9.3640(1)
b [Å]	10.2418(1)
c [Å]	4.5778(1)
α [°]	91.7588(2)
β [°]	94.7710(2)
γ [°]	83.5385(2)
V [Å^3]	434.63(1)
d_x [g cm^{-3}]	1.71
$F(000)$	232
Data range	$3.03 \leq 2\theta \leq 40.53°$; 7500 data points
No. of reflections	751
Temperature [K]	294
M_{20}	239
Refined parameters:	
structural	–
lattice	6
positional	42
displacement	4
Texture	14
Profile	28
Background	12
Zero-shift	1
GoF[a])	7.94 (12.7)
R_p [%][a])[b])	4.71 (7.09)
R_{wp} [%][a])[c])	6.75 (9.85)

[a]) Values in parentheses indicate the results of the full pattern-decomposition procedure ($3.03 \leq 2\theta \leq 28.03°$. [b]) $R_p = \Sigma\,|\,y_{obs} - y_{calc}\,|\,/\,\Sigma\,y_{obs}$. [c]) $R_{wp} = \{\Sigma\,(w \times (y_{obs} - y_{calc})^2)/\Sigma\,(w \times y_{obs}^2)\}^{1/2}$.

work are also different, and no transformation matrix could be found between our unit-cell data and those reported earlier by *Frazier et al.* [16]. The calculated density ($d_x =$ 1.71 g cm^{-3}), is in good agreement with the experimentally derived density ($d_m =$ 1.735 g cm^{-3}) determined by pycnometry.

The structure determination was carried out by a genetic algorithm. In the 'Search Molecule Position' module of the in-house-modified program MRIA [17], the initial melaminium orthophosphate (MP) model consisted of a melaminium trication (protonated at all endocyclic N-atoms) and a phosphate anion. These moieties were searched for independently, as discussed in the *Exper. Part.*

In view of the discussion above, no attempts were undertaken to perform a *Rietveld* refinement with melaminium cations having one or more protonated NH_2 groups. A *Rietveld* refinement was carried out using *a*) a neutral melamine molecule, *b*) the three monocations, *c*) the three dications, and *d*) the trication. Eventually, the *Rietveld* refinements were carried out without any distance restraints. The crystallographic R_p and R_{wp} values of the final models are not substantially different. For example, the

model with three protonated endocyclic N-atoms resulted in $R_p = 5.15\%$, $R_{wp} = 7.29\%$, and GoF (goodness of fit) 8.57, while the monocation model discussed hereafter resulted in lower – but comparable – consistency criteria ($R_p = 4.71\%$, $R_{wp} = 6.75\%$, GoF = 7.94). A detailed analysis of the trication structure, however, revealed too short intermolecular H···H distances of 1.24 and 1.49 Å, together with some relative short intermolecular O···O distances of 2.52 and 2.58 Å. The only crystal structure model found without too short intermolecular distances, discussed hereafter, consists of a melaminium cation with only *one* protonated melamine-ring N-atom and a $H_2PO_4^-$ anion.

The shortest P–O bond distance, d[P(1)–O(3)] = 1.475(2) Å (*Table 2*), for $H_2PO_4^-$ is substantially smaller than the remaining three ones (1.525(2)–1.593(2) Å), which indicates significant double-bond character. The H-atoms are considered to be bonded to O(4) and O(5), having the longest P–O distance. However, *Rietveld* refinement with a H-atom bonded to O(2) instead of O(5) resulted in nearly identical consistency parameters. The model with a H-atom bonded to O(5) is discussed hereafter, but it should be kept in mind that the total energy of the alternative model, as calculated with Cerius2 (Universal Force Field), is of comparable order of magnitude.

Table 2. *Selected Bond Distances* (in Å) *and Bond Angles* (in °) *of Melaminium Orthophosphate.* Estimated standard deviations are given in parentheses. Trivial atom numbering (see *Fig. 2*).

Triazene Moiety:			
C(12)–N(8)	1.402(3)	N(10)–C(14)	1.461(3)
N(8)–C(13)	1.305(3)	C(14)–N(9)	1.302(3)
C(13)–N(10)	1.358(3)	N(9)–C(12)	1.357(3)
C(12)–N(8)–C(13)	120.0(2)	N(10)–C(14)–N(9)	129.4(2)
N(8)–C(13)–N(10)	127.9(2)	C(14)–N(9)–C(12)	116.9(2)
C(13)–N(10)–C(14)	107.1(2)	N(9)–C(12)–N(8)	118.6(2)
Substituents:			
C(12)–N(6)	1.271(3)	C(14)–N(11)	1.359(3)
C(13)–N(7)	1.356(3)	N(8)–H(21)	0.995
N(8)–C(12)–N(6)	119.6(2)	N(10)–C(14)–N(11)	108.3(2)
N(9)–C(12)–N(6)	121.8(2)	N(9)–C(14)–N(11)	122.3(2)
N(8)–C(13)–N(7)	118.4(2)	C(12)–N(8)–H(21)	119.3
N(10)–C(13)–N(7)	113.7(2)	C(13)–N(8)–H(21)	120.6
H_2PO_4 Moiety:			
P(1)–O(2)	1.525(2)	P(1)–O(4)	1.575(2)
P(1)–O(3)	1.475(2)	P(1)–O(5)	1.593(2)
O(2)–P(1)–O(3)	119.35(10)	O(3)–P(1)–O(4)	109.43(9)
O(2)–P(1)–O(4)	106.02(9)	O(3)–P(1)–O(5)	110.03(9)
O(2)–P(1)–O(5)	105.79(9)	O(4)–P(1)–O(5)	105.28(9)

Several argumentations can be given why a second deprotonation of H_3PO_4 – leading to a melaminium dication and HPO_4^{2-} – will not take place. It was already mentioned (*vide supra*) that protonation of a second endocyclic N-atom of melamine is less favorable than protonation of the first one. The pK_a values of H_3PO_4 are 2.15, 7.21, and 12.34 for the first, second, and third deprotonation, respectively. $H_2PO_4^-$ is, therefore, too weak an acid for the second deprotonation to occur. The pK_a values of phosphorous acid (H_3PO_3) of 1.8 and 6.2 are somewhat lower. Nevertheless, in the

recently reported single-crystal structure of bis(melaminium) hydrogenphosphite tetrahydrate [18], only the mono-anion and cation are formed.

The model presented here was corroborated by solid-state NMR experiments [19]. Two-dimensional $^{1}H,^{13}C$-, $^{1}H,^{15}N$-, and $^{1}H,^{31}P$-correlation spectra all indicated a single H-atom coordinated to the endocyclic N-atom, and two H-atoms connecting pairs of orthophosphate units. Of the four main resonances in the ^{1}H-NMR spectrum of MP (*Fig. 1,a*), the two broad lines (δ(H) 4–10 ppm) stem from the NH_2 groups. The two other resonances appear above 10 ppm and are due to protons involved in H-bonding in a ratio of 2:1, *i.e.*, H-atoms bonded to the phosphate O-atoms and a H-atom bonded to an endocyclic N-atom, respectively.

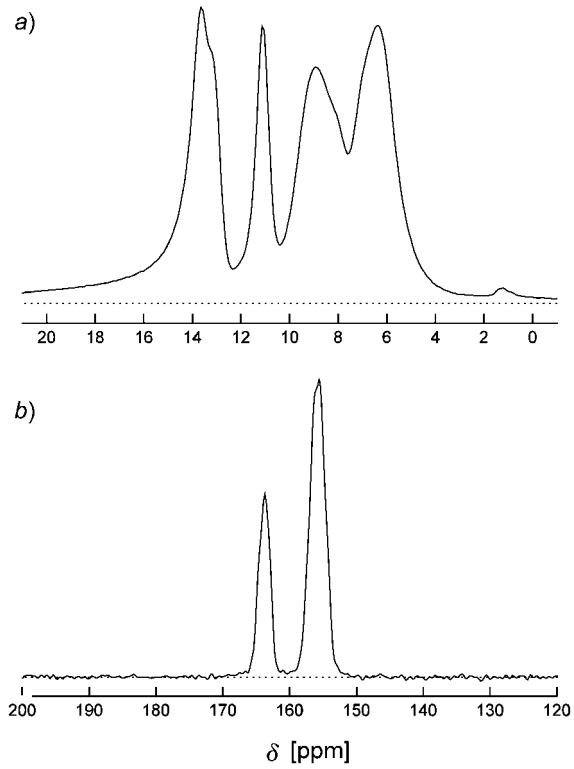

Fig. 1. a) *Single-pulse magic-angle-spinning solid-state ^{1}H-NMR spectrum of melaminium orthophosphate* (MP), *showing four main resonances.* The spectrum was obtained at a static field of 18.8 T, with a sample-spinning frequency of 49.1 kHz. b) *Cross-polarization magic-angle-spinning solid-state ^{13}C-NMR spectrum of MP.* The spectrum was obtained at a static field of 7.1 T, with a sample-spinning frequency of 12 kHz; the cross-polarization interval was 1.4 ms. TPPM Decoupling with a ^{1}H-nutation frequency of 100 kHz, pulse duration of 5 μs, and *rf* phases of $\pm 25°$ were applied during acquisition.

Two resonances (2:1) appear in the ^{13}C-NMR (CPMAS) spectra of MP (*Fig. 1,b*) instead of a single peak (as in pure melamine), indicating that the C-atoms in the melamine ring have become inequivalent, and being in line with protonation of an endocyclic N-atom. The ^{31}P-NMR spectrum displays a single line from the orthophos-

phate unit. A detailed discussion of the solid-state-NMR results will appear elsewhere [19].

The structure presented in this paper was used as a starting model in a combined *Rietveld*/quantum-mechanics procedure [20]. Simulated annealing performed with PowderSolve [21] was based on the lattice parameters and space-group symmetry of the present data. Omitting H-atoms, melamine and phosphate were considered as separate groups with three translational and three rotational degrees of freedom. Geometry optimizations were carried out with CASTEP, keeping the lattice parameters fixed and using the exchange-correlation functional of *Perdew*, *Burke*, and *Ernzerhof* (PBE) [22]. This led to a stable crystal structure similar to the one presented here [20].

2.3. *Molecular Structure.* Selected bond distances and angles are compiled in *Table 2*. The melaminium cation is singly protonated at an endocyclic N-atom (*Fig. 2*). The average ring and terminal C–N bond lengths are 1.364(7) and 1.329(5) Å, respectively. The six-membered ring exhibits significant distortions from the ideal hexagonal form. The internal C–N–C bond angle at the protonated ring N-atom (120.0(2)°) is significantly larger than the other two C–N–C angles of the ring (107.1(2) and 116.9(2)°). These differences are due to the steric effect of an electron lone pair, and are fully consistent with the valence-shell electron-pair-repulsion theory [23]. A similar correlation between the internal C–N–C angles of the melaminium ring is observed in the crystal structure of the co-crystal of barbituric acid with melamine [24], melaminium phthalate [25], and melaminium chloride hemihydrate [26]. As a result of the protonation of the endocyclic N-atom, the internal N–C–N angle, involving only nonprotonated ring N-atoms, is larger than those containing

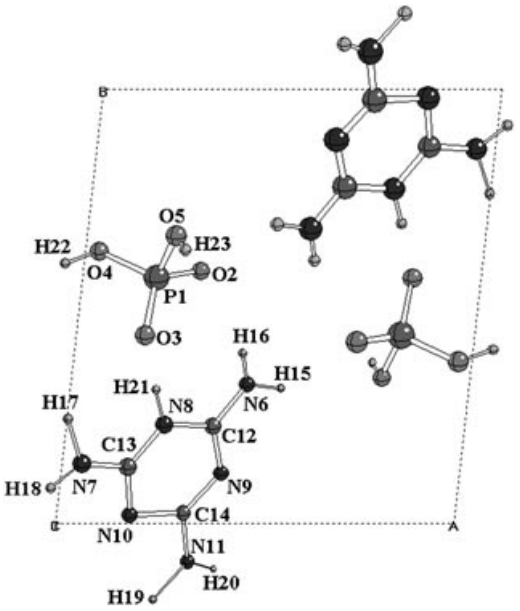

Fig. 2. *Structure and atom numbering of melaminium orthophosphate in the asymmetric part of the unit cell*

protonated and nonprotonated ring N-atoms. *Janczak* and *Perpétuo* [27] reported that the ring distortion of the melaminium residue mainly results from protonation, and, to a lesser degree, from H-bonding and crystal packing.

The bond lengths and angles in the melaminium moiety of MP are comparable to those found in other melaminium-monocation structures, with two exceptions. *1*) In all other known crystal structures, the internal N–C–N angle is invariably larger than 120°, while in the present case the N(8)–C(12)–N(9) bond angle is only 118.6(2)°. *2*) The exocyclic N–C–N angle at the side of the protonated ring N-atom is invariably smaller than at the nonprotonated ring N-atom; in MP, this angle is smaller at C(12), but larger at C(13) (*Table 2*).

The six-membered aromatic ring of the melaminium residue is almost planar, the maximum deviation of a nonhydrogen atom from the least-squares plane being 0.023(3) Å. The NH_2 groups are approximately coplanar with the least-squares plane through the melaminium ring, the angle of the least-squares plane through the amino group and the melaminium ring being 0.9(2), 3.8(2) and 0.8(1)° for N(6), N(7), and N(11), respectively.

2.4. *Crystal Lattice.* The crystal structure of MP consists of melaminium layers and pairs of orthophosphate chains, connected by H-bonds almost perpendicular to the layers (*Fig. 3*, *Table 3*). The orthophosphate chains are oriented parallel to the *c*-axis, while the melaminium layers are parallel to the (1 – 1 1) plane (*Fig. 4*,*a*). The distance between melaminium layers is 3.62 Å, slightly larger than the distance of *ca.* 3.4 Å between aromatic layers that display π/π interactions [28]. Neighboring melaminium molecules do not lie in the same plane, but in two parallel planes at close distance (0.79 Å), and are shifted with respect to each other. Furthermore, these melaminium layers are slightly tilted with respect to the planes that can be drawn through the centers

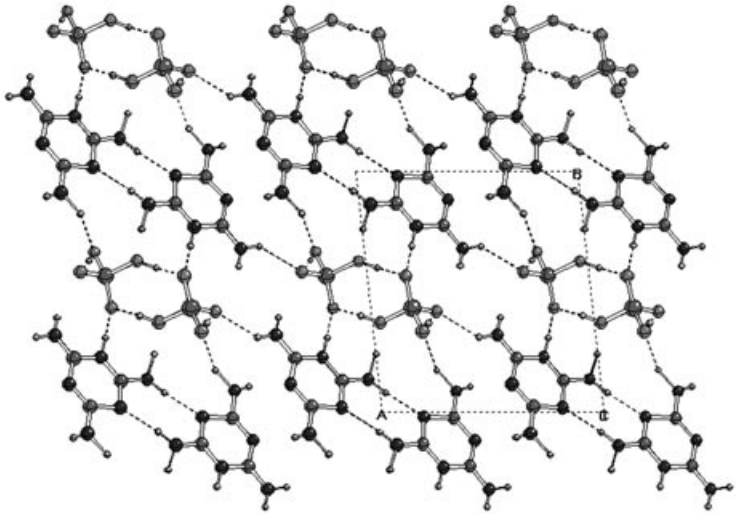

Fig. 3. *Crystal packing of melaminium orthophosphate viewed along the* c*-axis.* The *a*-axis runs horizontally.

Table 3. *Crystallographically Identified H-Bonds in Melaminium Orthophosphate* (MP). The letters 'D' and 'A' represent 'donor' and 'acceptor', respectively. For atom numbering, see *Figs. 2* and *5*.

D–H···A	D–H [Å]	H···A [Å]	D···A [Å]	D–H–A [°]	Symmetry operation
N(6)–H(15)···O(2)	0.97	2.06	2.849(2)	137	$1-x, 1-y, 1-z$
N(6)–H(16)···O(2)	0.97	2.13	3.019(2)	151	$x, y, 1+z$
N(7)–H(17)···O(4)	0.96	2.56	3.485(2)	161	$-x, 1-y, 2-z$
N(7)–H(17)···O(5)	0.96	2.60	3.142(2)	116	$-x, 1-y, 2-z$
N(7)–H(18)···N(10)	0.97	1.94	2.862(3)	157	$-x, -y, 2-z$
N(11)–H(19)···O(5)	0.96	1.98	2.893(2)	157	$x, -1+y, z$
N(11)–H(20)···N(9)	0.97	2.05	3.018(3)	178	$1-x, -y, 1-z$
N(8)–H(21)···O(3)	0.99	1.80	2.780(2)	169	$x, y, 1+z$
O(4)–H(22)···O(3)	1.06	1.52	2.582(2)	177	$-x, 1-y, 1-z$
O(5)–H(23)···O(2)	1.01	1.51	2.515(2)	179	$x, y, 1+z$

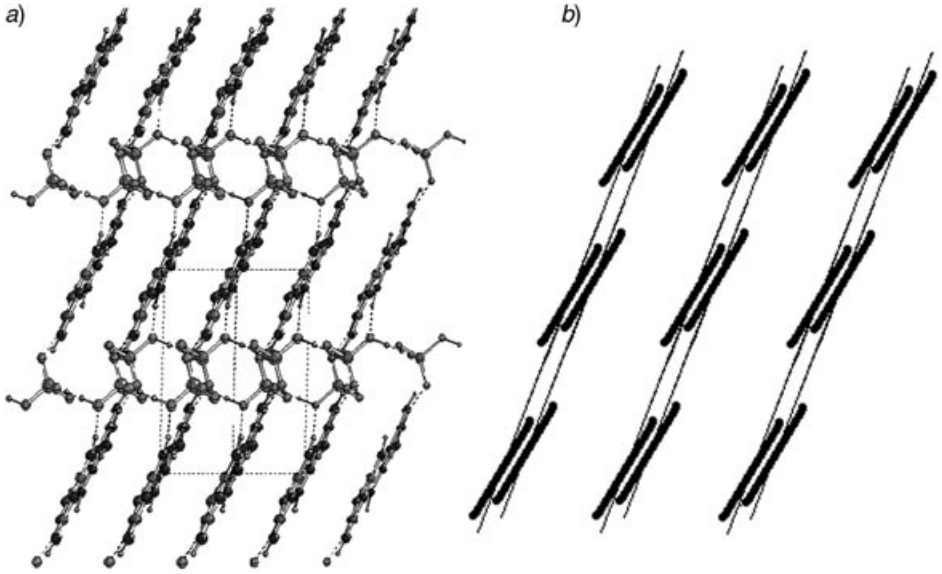

Fig. 4. a) *Unit cell of melaminium orthophosphate viewed along [1 0 1], showing the stacking of the melaminium layers*; *and* b) *simplified projection of the melaminium molecules with respect to the plane through their centers, showing that two neighboring melaminium molecules are not coplanar*

of the molecules (*Fig. 4*). The orthophosphate chains are connected by both intra-chain and inter-chain H-bonds (*Fig. 5*).

3. Outlook. – The results presented in this paper show that, in the absence of suitable single crystals, a good structure determination can be obtained from high-resolution powder-diffraction data using the high intensity of a synchrotron source. The ease of solving crystal structures from powder-diffraction data is no longer restricted to small, fairly rigid, (in)organic molecules like the moieties presented here. Indeed, in the last few years, structures of much larger and more flexible molecules have been solved

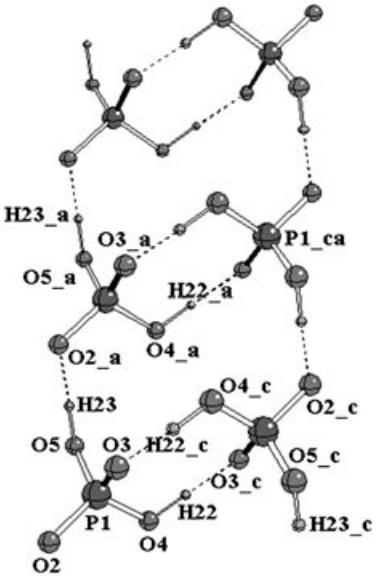

Fig. 5. *Pairs of phosphate chains* (in vertical direction) *in melaminium orthophosphate.* P=O and P–O Bonds are shown as black and white sticks, respectively. Subscripts _a, _c and _ca correspond to symmetry operations $(x, y, 1+z)$, $(-x, 1-y, 1-z)$, and $(-x, 1-y, 2-z)$, respectively.

in our laboratory, *e.g.*, the inclusion complex of β-cyclodextrin with mefenamic acid [29].

Heating melaminium orthophosphate at 240° during at least 2 h results in dehydratation and the formation of melaminium pyrophosphate. The structure of this compound was also established by high-resolution synchrotron powder-diffraction data and will be discussed in the near future by *Brodski et al.* [30].

Experimental Part

Synthesis. Melaminium orthophosphate (MP) was prepared at *DSM* (Geleen, The Netherlands) by heating a mixture of melamine (63.060 g, 0.5 mol) with H_2O (250 ml) to 75°. Under vigorous stirring, H_3PO_4 (48.998 g, 0.5 mol) was added to this mixture, which was stirred for 2 h at 75°. The solvent was evaporated *in vacuo* at 80°, affording MP as a white solid.

X-Ray Crystal-Structure Determination. Initially, MP was subjected to measurements on an *Enraf-Nonius Guinier-Johansson* camera equipped with a *Johansson* monochromator, using CuKα_1 radiation ($\lambda = 1.54060$ Å) at 294 K. The sample was prepared by pressing the MP powder to a thin layer onto *Mylar* foil. To improve particle statistics, the sample holder was rotated in the specimen plane during exposure. For indexing, the accurate positions of 54 lines in the interval $2\theta = 0.0 - 40.0°$ were collected by reading out the *Guinier* photograph with an in-house-built optical instrument. The lines were indexed with the program ITO [31], with a Figure of Merit of $M_{20} = 75$. A number of weak lines could not be indexed, indicating the presence of some trace contamination (1–2%).

For complete structure elucidation, a capillary of diameter 1.5 mm was filled with MP powder and measured at the high-resolution powder station of BM01B of the Swiss–Norwegian Collaborating Research Group at the *European Synchrotron Radiation Facility* (ESRF, Grenoble, France), with $\lambda = 0.75003$ Å, and at 294 K. The diffractometer was equipped with six detectors (Na-I scintillation counter). The capillary was rotated during exposure. Continuous scans were made from 3.03° to 43.25° (2θ) and binned finally at a step size

of 0.005°. To obtain reflection intensities, X_{obs} [32], a full pattern decomposition was carried out with the program MRIA [17], using a split-type pseudo-*Voigt* peak-profile function [33]. It was applied to the $2\theta = 3.03 - 28.03°$ region, resulting in $R_p = 7.09\%$, $R_{wp} = 9.85\%$, and GoF = 12.71. The initial molecular model for MP was created by taking melaminium (REFCODE ZENWEU: melaminium diperchlorate hydrate [34]) and phosphate models (REFCODE ZIDNAB: tetrakis(guanidinium) phosphate chloride dihydrate [35]) from the *Cambridge Structural Database* [16]. ZENWEU Melaminium is a dication, and was modified into a trication. To position both moieties in the asymmetric part of the unit cell, a locally modified version of a grid-search procedure [32] was applied to a set of 50 low-order X_{obs} reflections obtained from the full pattern decomposition. Instead of the classical grid-search procedure [32], a genetic algorithm [36] was used to perform the translational and rotational search in the asymmetric unit. In this process, the melaminium and phosphate moieties can be searched for independently. This procedure resulted in an exceptionally low $R(X)$ value [32] of 10.6%.

The model found in this way was refined using the *Rietveld* module of MRIA [17], with a split-type pseudo-*Voigt* peak-profile function [33]. The preferred orientation was refined with the symmetrized-harmonics expansion method [37]. *Rietveld* refinement was applied to the region $2\theta = 3.03 - 40.53°$. Initially, (soft) distance restraints on all bonds and nonbonding distances < 3.0 Å were applied, as well as a small damping factor to improve the convergence of the refinement. At the later refinement stages, the restraints could be removed completely. H-atoms were introduced at their calculated position and not refined. U_{iso} Values of identical atom types were coupled during the refinement. Plots of observed and calculated X-ray diffraction patterns, and a difference plot after *Rietveld* refinement, are depicted in *Fig. 6*.

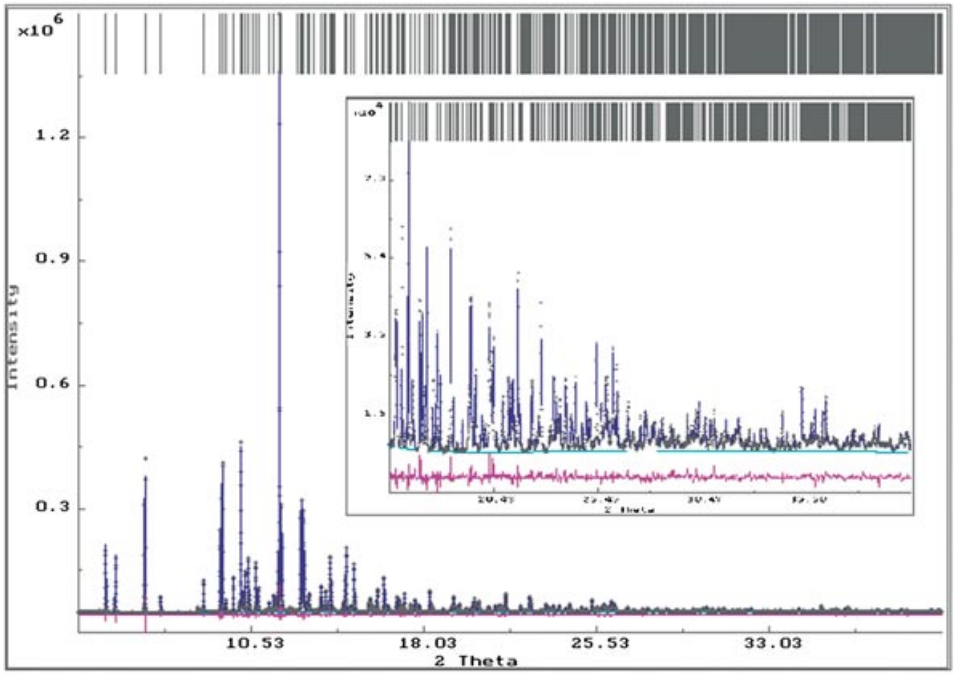

Fig. 6. *Full-range high-resolution synchrotron powder-diffraction pattern of melaminium orthophosphate.* The representation shows the experimental pattern (black dots), the calculated pattern after final *Rietveld* refinement (blue line), the calculated background (light blue line), and the difference pattern (experimental – calculated; pink line). Markers of all reflections are included. The inserted figure shows the high-angle range of the pattern. The patterns were recorded at 0.75003-Å wavelength.

CCDC-224290 contains the supplementary crystallographic data for this paper. These data can be obtained, free of charge, *via* www.ccdc.cam.ac.uk/conts/retrieving.html or from the *Cambridge Crystallographic Data Centre*, 12 Union Road, Cambridge CB2 1EZ, UK (fax: +44-1223-336-033; e-mail: deposit@ccdc.cam.ac.uk).

The authors gratefully acknowledge *DSM* (Geleen, The Netherlands) and *Ciba Specialty Chemicals* (Basel, Switzerland) for the preparation of the MP sample and for financial support, *Ed Sonneveld* (Laboratory for Crystallography, van't Hoff Institute for Molecular Sciences, University of Amsterdam) for collecting the *Guinier* powder-diffraction data and indexing the *Guinier* pattern, and Ing. *Wouter van Beek* from BM01B at the *European Synchrotron Radiation Facility* (Grenoble, France) for his help during the high-resolution powder-diffraction measurements. The authors gratefully acknowledge Prof. *Arno Kentgens*, Dr. *Andreas Brinkmann*, Dr. *Ernst van Eck*, and *Adri Klaassen* (Physical Chemistry/Solid State NMR, University of Nijmegen, The Netherlands) for providing the results of the solid-state NMR experiments prior to publication, and *Ad Braam*, *Betty Coussens*, *Shahab Jahromi*, *Victor Litvinov* (all *DSM*/*Ciba Specialty Chemicals*), and *Rob Helmholdt* (Laboratory for Crystallography, van 't Hoff Institute for Molecular Sciences, University of Amsterdam) for helpful discussions.

REFERENCES

[1] J. de Boer, P. G. Wester, H. J. C. Klamer, W. E. Lewis, J. P. Boon, *Nature (London)* **1998**, *394*, 28; A. Shanley, *Chem. Eng.* **1998**, *105*, 61.
[2] S. Jahromi, U. Moosheimer, *Macromolecules* **2000**, *33*, 7582; S. Jahromi, W. Gabriëlse, A. Braam, *Polymer* **2003**, *44*, 25.
[3] A. Ranganathan, V. R. Pedireddi, C. N. R. Rao, *J. Am. Chem. Soc.* **1999**, *121*, 1752.
[4] B. Bann, S. A. Miller, *Chem. Rev.* **1958**, *58*, 131; A. W. Frazier, J. Gautney, J. L. Cabier, *Ind. Eng. Chem. Prod. Res. Dev.* **1982**, *21*, 470.
[5] V. S. I. Volfkovic, W. Feldmann, M. L. Kozmina, *Z. Anorg. Allg. Chem.* **1979**, *20*, 20.
[6] R. C. Hirt, R. G. Schmitt, *Spectrochim. Acta* **1958**, *12*, 127.
[7] G. Morimoto, *Rev. Phys. Chem. Jpn.* **1967**, *37(1)*, 54.
[8] T. N. Roginskaya, A. I. Finkelstein, *Russ. J. Phys. Chem.* **1971**, 913 (*Zurnal Fizicheskoi Khimii* **1971**, *45*, 1609).
[9] A. Albert, R. Goldacre, J. Phillips, *J. Chem. Soc.* **1948**, 2240.
[10] B. A. Korolev, M. A. Mal'tseva, *Zhurnal Obshchei Khimii* **1976**, *46(7)*, 1605.
[11] K. Inuzuka, R. Shiba, M. Tajima, *Netsu Kokasei Jushi* (*J. Thermosetting Plastics*) **1983**, *4*, 1.
[12] R. Bacaloglu, I. Bacaloglu, Z. Simon, *Rev. Roum. Chim.* **1992**, *37*, 819.
[13] A. I. Finkelstein, T. N. Roginskaya, L. A. Simkina, *Izv. Vyssh. Uchebn. Zaved., Khim. Khim. Tek.* **1994**, *37*, 51.
[14] D. V. Jahagirdar, R. M. Kharwadkar, *Indian J. Chem., Sect. A* **1981**, *20*, 635.
[15] F. H. Allen, O. Kennard, *Chem. Des. Autom. News* **1993**, *8*, 31.
[16] A. W. Frazier, K. R. Waerstad, Y. K. Kim, *J. Chem. Eng. Data* **1988**, *33*, 518.
[17] V. B. Zlokazov, V. V. Chernyshev, *J. Appl. Crystallogr.* **1992**, *25*, 447.
[18] L. E. Gordon, W. T. A. Harrison, *Acta Crystallogr., Sect. E* **2003**, *59*, 195.
[19] A. Brinkmann, E. R. H. van Eck, A. A. K. Klaassen, A. P. M. Kentgens, in preparation.
[20] B. Coussens, *DSM*/*Ciba Specialty Chemicals*, Geleen, The Netherlands, personal communication.
[21] G. E. Engel, S. Wilke, O. König, K. D. M. Harris, F. J. J. Leusen, *J. Appl. Crystallogr.* **1999**, *32*, 1169.
[22] J. P. Perdew, K. Burke, M. Ernzerhof, *Phys. Rev. Lett.* **1996**, *77*, 3865.
[23] R. J. Gillespie, *J. Chem. Educ.* **1963**, *40*, 295; R. J. Gillespie, *Chem. Soc. Rev.* **1992**, *21*, 59.
[24] J. A. Zerkowski, J. C. McDonald, G. M. Whitesides, *Chem. Mater.* **1994**, *6*, 1250.
[25] J. Janczak, G. J. Perpétuo, *Acta Crystallogr., Sect. C* **2001**, *57*, 123.
[26] J. Janczak, G. J. Perpétuo, *Acta Crystallogr., Sect. C* **2001**, *57*, 1120.
[27] J. Janczak, G. J. Perpétuo, *Acta Crystallogr., Sect. C* **2001**, *57*, 873.
[28] L. Pauling, 'The Nature of the Chemical Bond', 3rd edn., Cornell University Press, Ithaca, 1960, p. 262.
[29] M. M. Pop, K. Goubitz, G. Borodi, M. Bogdan, D. J. A. De Ridder, R. Peschar, H. Schenk, *Acta Crystallogr., Sect. B* **2002**, *58*, 1036.
[30] V. Brodski, R. Peschar, H. Schenk, A. Brinkmann, E. R. H. van Eck, A. P. M. Kentgens, B. Coussens, A. Braam, in preparation.
[31] J. W. Visser, *J. Appl. Crystallogr.* **1969**, *2*, 89.

[32] V. V. Chernyshev, H. Schenk, *Z. Kristallogr.* **1998**, *213*, 1.
[33] H. Toraya, *J. Appl. Crystallogr.* **1986**, *19*, 440.
[34] A. Martin, A. A. Pinkerton, *Acta Crystallogr., Sect. C* **1995**, *51*, 2174.
[35] M.-T. Averbuch-Pouchot, A. Durif, *C. R. Seances Acad. Sci., Ser. II* **1993**, *317*, 1179.
[36] R. A. J. Driessen, Faculty of Science, University of Amsterdam, unpublished results.
[37] M. Ahtee, M. Nurmela, P. Suortti, M. Järvinen, *J. Appl. Crystallogr.* **1989**, *22*, 261; M. Järvinen, *J. Appl. Crystallogr.* **1993**, *26*, 525.

Received February 24, 2004